MULTI-SPACECRAFT OBSERVATIONS OF INTERPLANETARY SHOCK ACCELERATED PARTICLE EVENTS

G. C. Ho[1], D. Lario[1], R. B. Decker[1], M. I. Desai[2], Q. Hu[3], J. Kasper[4], A.-F. Viñas[5]

[1] The Johns Hopkins University Applied Physics Laboratory, Laurel, MD 20723, USA, Email:George.Ho@jhuapl.edu
[2] Southwest Research Institute, San Antonio, TX 78228, USA
[3]Institute of Geophysics and Planetary Physics, University of California, Riverside, CA 92521, USA
[4]Center for Space Research, MIT, Cambridge, MA 02139, USA
[5]Laboratory for Solar and Space Physics, NASA/GSFC, Greenbelt, MD 20771, USA

ABSTRACT

We use simultaneous measurements from the Wind and ACE spacecraft to determine the spatial properties of both interplanetary (IP) shocks and the shock-associated energetic particle events. We combine plasma, magnetic field and energetic particle data from ACE and Wind during five energetic storm particle (ESP) events and examine the spatial and temporal variations of these events in the Earth's vicinity. We find that even though the two spacecraft were separated by more than 300 R_E, the plasma, field, and particle data profiles during the events were very similar. We also used the fitted shock velocity along the normal from ACE and estimated the shock transit time to Wind location. In general, there is poor agreement between the estimated transit time and the actual measured transit time. Hence, our assumptions that a) the IP shock at 1 AU propagates radially, and/or b) the IP shock is spherically symmetric at 1 AU are not valid.

1. INTRODUCTION

Particle signatures of energetic storm particle (ESP) events have been studied since they were first discovered in the 1960s. Lee (1983) modeled energetic particle acceleration in ESP events with Fermi acceleration of solar wind ions at quasi-parallel shocks. In this model, ions streaming upstream of the shock drive hydromagnetic wave growth, and the resultant waves scatter the particles back and forth across the shock, yielding a small net energy gain on each cycle. In the shock drift model by Decker (1983), particles encounter the shock surface only once, gaining energy by drifting along the shock surface in the direction of the convection electric field. Both models predict ion spectra and anisotropies in the upstream and downstream regions of the shock. Using the low-energy (<1 MeV) particle detectors on ISEE-3, Sanderson *et al*. (1985) analyzed ion anisotropies in several ESP events and found cases that were consistent with both acceleration models. Although there have been many studies of ESP events with single spacecraft measurements, there have been no systematic studies devoted to understanding the structure and propagation of ions in ESP events near Earth using two or more spacecraft.

The location of ACE at the L1 Lagrangian point ~230 R_E upstream of the Earth ensures its continued exposure to IP shocks and their upstream regions. This has already provided us with a rich data set that allows detailed tests of shock acceleration theory (Lario *et al.* 2005a). However, with ACE we can only obtain single point measurements of ESP events, whereas to understand the spatial and temporal structure of IP shocks and ESP events, we need measurements at more than one location. Fortunately, the Wind spacecraft has been in operation since November 1994 (Acuña *et al.,* 1995), in a complex orbit which keeps it generally outside the magnetosphere between the Earth and L1. This has provided us with a critical second point measurement. Using data from highly sophisticated plasma, field, and energetic particle sensors on board ACE and Wind we have examined the global structure of IP shocks and ESP events between L1 and Earth. Such a comprehensive survey could not have been carried out prior to the 1990s. The acceleration processes, and therefore the characteristics of the associated ESP events, depend very sensitively on the shock strength and upstream geometry. The observation of the same traveling shock by two different spacecraft allows us to determine the properties of the shock propagation and its effect on the energetic particle intensities.

2. ENERGETIC PARTICLES

Lario *et al.* (2005b) and Ho *et al.* (2005) classified 191 ESP events from February 1998 to October 2003 on ACE according to both their time-intensity profiles and energy spectra. Detailed description of these events can be found in Ho *et al.* (2005). Out of these 191 shocks, 128 shocks were also detected at Wind when it was outside the

Proc. Solar Wind 11 – SOHO 16 "Connecting Sun and Heliosphere", Whistler, Canada
12 – 17 June 2005 (ESA SP-592, September 2005)

Earth's magnetosphere. Fig. 1 shows the locations of both ACE and Wind for all these 128 IP shock events.

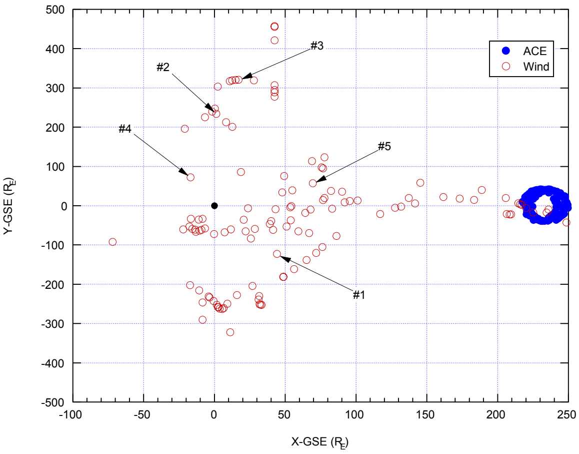

Figure 1. Location of ACE (blue) and Wind (red) for the 128 common shock events in the GSE X-Y plane.

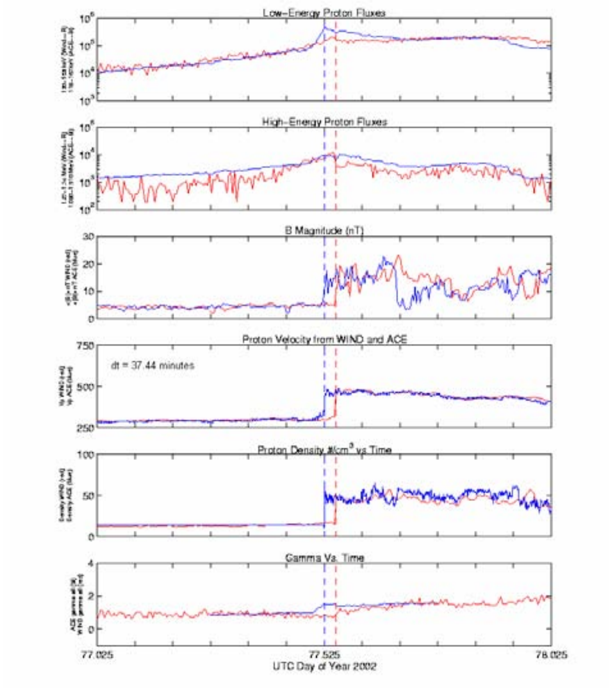

Figure 2. The figure shows the data from ACE (blue) and Wind (red). Particle data (~100 keV and ~1.5 MeV) of Event #1 are shown in the top two panels of the figure. The next three panels show the magnitude of the magnetic field, solar wind velocity, and density. The bottom panel shows the fitted power law indices of the ion energy spectra (200 keV – 2 MeV) on both ACE and Wind.

As discussed earlier, ACE is stationed at the L1 Lagrangian point ~230 R_E upstream of the Earth while Wind orbited many of the near-Earth geospace during the same time period. At times, they were separated by more than 400 R_E. We selected five of these common events for further study, as listed in Table 1. With the exception of Event #2, all the IP shocks were followed by the interplanetary counterparts of coronal mass ejections (ICMEs) as identified by Cane and Richardson (2003). Therefore, ACE and Wind intercepted the shock on day 113 (Event #2) near one of its flanks and far from its nose. Figs. 2 and 3 show the particle, magnetic field, and plasma data from both ACE (blue) and Wind (red) for Event #1 and #4, respectively. The dashed lines indicate when the shock traversed ACE and Wind. The time-intensity profiles measured by two similar energy channels (~100 keV and ~1.2 MeV) are shown in the first two panels. The magnetic field magnitude, solar wind velocity and density are shown in the next three panels, respectively. It is striking that despite the large separation (>300 R_E) between the two spacecraft, all quantities exhibited remarkably similar behavior. More importantly, after accounting for the time-shift, the particle spectral indices that were computed by fitting power law functions to the ion energy spectra (200 keV – 2 MeV) were also similar.

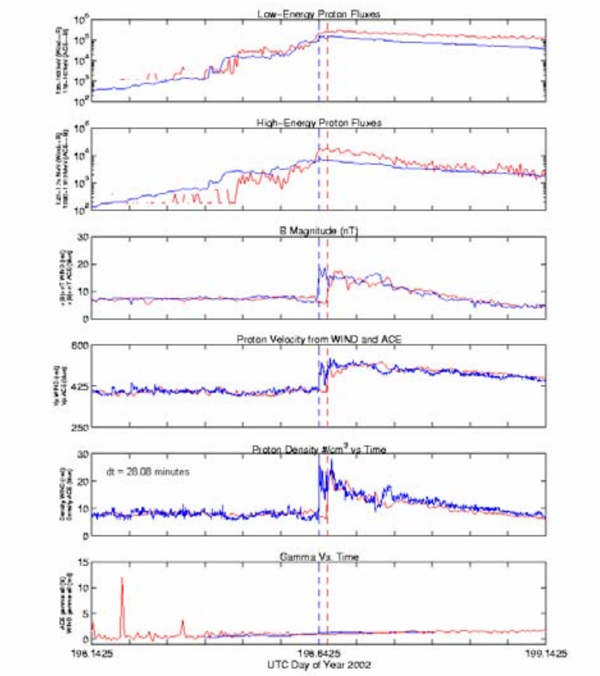

Figure 3. Particle, plasma and field data for Event #4. Same format as in Fig. 2.

The remaining three events (not shown) were also separated by more than ~300 R_E and yet they too

Table 1: List of selected 5 IP shock events in this study

Event Number	Year, DOY	Shock Arrival Time at ACE (UT)	Shock Arrival Time at Wind (UT)	Wind Location at GSE System (R_E)			Shock Speed at ACE (km/s)	Measured Transit Time (min)	Estimated Transit Time (min)
				X	Y	Z			
1	2002, 077	1237	1314	44.2	-122.7	-3.7	410±30	37.1	46.1±3.4
2	2002, 113	0415	0500	1.35	233.9	11.7	400±41	45.3	59.2±6.1
3	2002, 143	1015	1045	17.1	320.8	22.9	834±82	29.9	28.1±2.8
4	2002, 198	1526	1556	-16.9	72.5	4.0	493±40	29.7	56.9±4.6
5	2002, 250	1609	1622	69.5	56.7	5.2	628±40	13.2	26.6±1.7

exhibited remarkably similar energetic particle time-intensity profiles at ACE and Wind.

3. SHOCK PROPERTIES

For 156 of the 191 shocks ACE detected, we calculated both the shock velocity along the shock normal in the upstream frame of reference, V_s, and the density compression ratio, r_n (Ho *et al.,* 2005). The ACE shock parameters were obtained by employing the non-linear least-squares technique of Viña and Scudder (1986) to simultaneously solve the complete set of Rankine-Hugoniot relations for pairs of upstream and downstream data points (also see Ho *et al.,* 2005). The parameters for the shocks at Wind can be found in Kasper *et al.* (2005). Fig. 4 shows the density compression ratios for 108 common shocks at ACE and Wind (fitted slope l = 0.87±0.03). The solid line represents a unique compression ratio at the two spacecraft. Fig. 5 shows the shock speed as measured in the spacecraft frame from both ACE and Wind (fitted slope l = 0.79±0.01). In

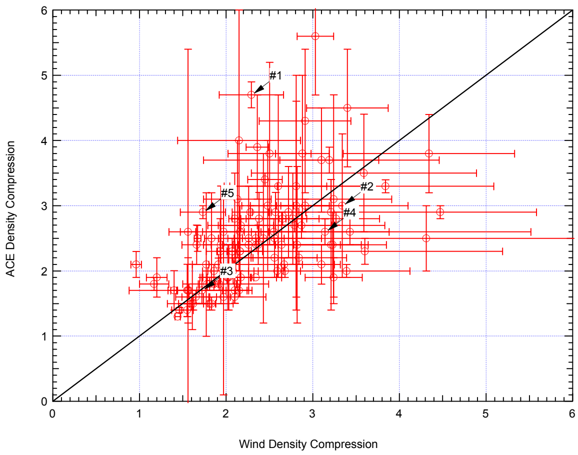

Figure 4. Density compression ratios for 108 interplanetary shocks that both ACE and Wind observed. The solid line indicates shocks with unique compression ratios at ACE and Wind.

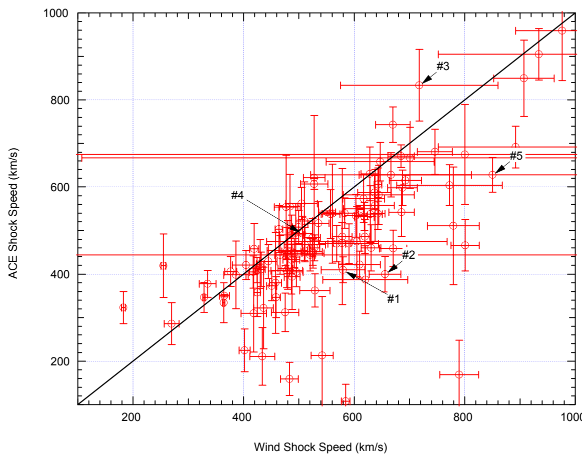

Figure 5. Shock velocity along the normal for 108 interplanetary shocks that both ACE and Wind observed. The solid line indicates shocks with the same velocity at ACE and Wind.

general, there is good agreement between the values measured by the two spacecraft.

4. SHOCK PROPAGATION

We estimated the shock transit time from ACE to Wind by assuming that a planar shock propagates radially along the X_{GSE} direction with a speed given by the fitted shock velocity along the normal on ACE. Although there is large variance in the directions of the shock normals, the assumption of radial propagation is reasonable since it has been found that on average the shock normals are indeed directed along the radial direction (Volkmer and Neubauer, 1985; Chao and Chen, 1985). Table 1 shows the comparison of the estimated transit time and the actual measured time on Wind. In the five cases we studied, there is generally a poor agreement between the two values. Fig 6 shows a comparison of the estimated and actual transit times for all the common shocks that were observed at ACE and Wind. The correspondence between the estimated and actual transit delays is reasonable up to 30 minutes, or when the separation between ACE and Wind is <100 R_E. In contrast, the correlation becomes significantly poor when the Y_{GSE} separation between ACE and Wind were greater than 200 R_E.

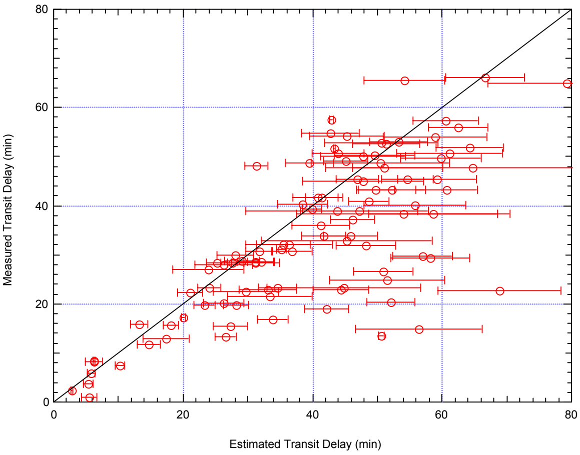

Figure 6. Estimated transit delays based on fitted ACE shock speed and the X_{GSE} separation. The solid line indicates when the value on ACE and Wind agrees with each other.

5. SUMMARY

We studied 128 IP shocks that were observed both by ACE and Wind from 1998 to 2003. We selected five events for detailed study. The plasma, magnetic field and particle data in these five events had similar time profiles even though at times they were separated by more than 300 R_E. We compared the fitted shock speed and density compression ratio at ACE and Wind for 108 events. In general, there is relatively good agreement between the two spacecraft. We then used the fitted shock speed on ACE and assumed a planar radially propagating shock to estimate the transit delay between ACE and Wind. The agreement between the estimated transit delay and the measured delay is reasonable up to < 30 minutes or <100 R_E separation. The disagreement increases when the Y_{GSE} separation was >200 R_E. This implies that (a) the shock may not be spherically symmetric at 1 AU, and/or (b) the shock did not propagate radially. Szabo (2005) studied shock properties by using only the measured shock arrival times and locations of four different spacecraft for a few IP shocks. On the basis of poor correlations similar to the ones reported here, Szabo concluded that IP shocks at 1 AU have curvature (or even corrugated surface) on the order of the separation between the spacecraft.

6. ACKNOWLEDGMENTS

The work at JHU/APL was supported under NASA grants NAG5-10836 and NNG04GA84G.

7. REFERENCES

Acuña M.H. et al., The Global Geospace Science program and its investigations, *Space Science Rev.,* 71, 5-21, 1995.

Cane H.V., and Richardson I.G., Interplanetary coronal mass ejections in the near-Earth solar wind during 1996-2002, *J. Geophys. Res.,* 108, SSH 6-1, CitID 1156, DOI 10.1029/2002JA009817, 2003.

Chao, J.K., and Chen Y.H., On the distribution of theta_Bn for shocks in the solar wind, *J. Geophys. Res.,* 90, 149-153, 1985.

Decker R.B., Formation of shock-spike events at quasi-perpendicular shocks, *J. Geophys. Res.,* 88, 9959-9973, 1983.

Ho G.C. et al. Transient shocks and associated energetic particle distribution observed by ACE during solar cycle 23, *J. Geophys. Res.,* submitted, 2005.

Kasper J. et al., *J. Geophys. Res.,* submitted, 2005.

Lee M.A., Coupled hydromagnetic wave excitation and ion acceleration at interplanetary travelling shocks, *J. Geophys. Res.,* 88, 6109-6119, 1983.

Lario D. et al., ACE observations of energetic particles associated with transient interplanetary shocks, in *Solar Wind Ten,* ed. M. Velli et al., American Institute of Physics, CP679, 640-643, 2003.

Lario D. et al., The energetic storm particle event on 2003 October 24: A test of diffusive acceleration theory, *Proc. Of the 4th IGPP-UCR Annual International Astrophysics Conference on the Physics of Collisionless Shocks,* in press, 2005a.

Lario D. et al., Statistical properties of fast forward transient interplanetary shocks and associated energetic particle events: ACE observations. *Proc. Of the 11th Int. Solar Wind Conf.,* this issue, 2005b.

Sanderson T.R., Reinhard R., van Nes P. and Wenzel K.-P., Observations of three-dimensional anisotropies of 35- to 1000-keV protons associated with interplanetary shocks, *J. Geophys. Res.,* 90, 19-27, 1985.

Szabo A., Determination of the properties of interplanetary shocks, *SHINE 2005 Workshop,* 2005.

Volkmer P.M., and Neubauer, F.M., Statistical properties of fast magnetoacoustic shock waves in the solar wind between 0.3 AU and 1 AU: Helios-1, 2 observsations, *Annales Geophysicae,* 1, 1-12, 1985.

Viñas A.F-., and Scudder, J.D. Fast optimal solution to the "Rankine-Hugoniot problem:, *J. Geophys. Res.,* 91, 39-58, 1986.